NASA CONTRACTOR REPORT

NASA CR-1512

N·A·S·A·CR-15

c.1

LAUNCH VEHICLE ERROR SENSITIVITY STUDY

by Richard C. Rosenbaum and Robert E. Willwerth

Prepared by
LOCKHEED MISSILES & SPACE COMPANY
Sunnyvale, Calif.
for Langley Research Center

NATIONAL AERONAUTICS AND SPACE ADMINISTRATION • WASHINGTON, D. C. • FEBRUARY 1970

LAUNCH VEHICLE ERROR SENSITIVITY STUDY

By Richard C. Rosenbaum and Robert E. Willwerth

FOREWORD

This report was prepared by the Research and Development Division of the Lockheed Missiles and Space Company, Sunnyvale, California. It presents the results of a study made for the Langley Research Center under NASA contract NAS1-8920. The work was administered under the direction of Dr. John D. Bird of the Astromechanics Branch at LRC.

Dr. Richard C. Rosenbaum and Mr. Robert E. Willwerth are responsible for the work presented here. Computer programming was performed by Miss Zoe Taulbee. This work was aided by several illuminating discussions with Prof. John V. Breakwell of Stanford University.

ABSTRACT

A method is presented for shaping a booster trajectory to minimize the sensitivity of terminal constraints to variations in vehicle or atmosphere parameters. An example, using the Scout booster, is given in which it is shown that the sensitivity of terminal altitude to variations in first stage burn rate can be reduced by 50%. An investigation, using trial and error techniques, is also made to examine the influence of the trajectory shape on some of the other major error sources for the Scout vehicle.

TABLE OF CONTENTS

LIST OF SYMBOLS

a   weighting functions for system variables

A   booster reference area

A_e nozzle exit area

b   weighting functions for system parameters

C_D drag coefficient

f   vector of derivatives

F $\dot{v}$

g   gravitational acceleration

g_o gravitational acceleration at sea level

G $\dot{\gamma}$

h   altitude

I $\dot{r}$

I_{sp} specific impulse

K $\dot{\tau}$

m   mass

N $\dot{m}$

p   atmospheric pressure

P   vector of system variables

q   vector of system parameters

r   radius

S   sensitivity of ψ to q

s_q weighted sum of components of S

S_ϕ change in payoff ϕ due to unit change in parameter τ

t   time

T   thrust

v   velocity

x   vector of state variables

α vector of control variables

γ flight path angle

θ thrust attitude angle measured with respect to inertial coordinate system

λ_ψ vector of adjoint variables associated with constraint ψ

Λ_p weighted sum of components of Λ_ψ

Λ_ϕ influence coefficient relating α to ϕ

Λ_ψ influence coefficient relating P to ψ

μ vector of adjoint variables associated with λ

μ gravitational constant when used in equations of motion

ν vector of adjoint variables associated with the sensitivity payoff

ρ atmospheric density

τ vector of control parameters

τ longitude when used in equations of motion

ϕ payoff

ψ terminal constraint

LAUNCH VEHICLE ERROR SENSITIVITY STUDY

by

Richard C. Rosenbaum and Robert E. Willwerth

Lockheed Missiles and Space Company

SECTION 1

INTRODUCTION

The advent of the high speed digital computer, together with the
development of the gradient method of trajectory optimization, has made
it possible to rapidly determine the maximum performance of booster
vehicles. In many cases, however, the capability of the booster exceeds
the mission requirements. The payload to be placed in orbit, for example,
may weigh considerably less than the maximum payload that the booster
can deliver into orbit. A variety of trajectories will satisfy the
mission requirement. It is logical to inquire whether the excess
booster capacity can be used to improve some characteristic of the tra-
jectory.

In this report, a method is presented for using the excess booster
capability to shape the trajectory in order to reduce the sensitivity
of the terminal constraints to variations in booster or atmosphere para-
meters. This is particularly important if an open-loop guidance system
is being used because there is no way to correct the pitch program to
compensate for non-standard conditions.

Trajectory shaping to minimize sensitivity has been employed in
references 1 and 2. Leondes and Volgenau in reference 1 reduce the impact
error of a ballistic missile by finding a trajectory which minimizes the

1

weighted sum of the partial derivatives of range with respect to the state variables at burnout. A significant reduction in sensitivity is reported. Watson and Stubberud in reference 2 attempt to reduce the effect of atmospheric density variations on the impact point of an entry vehicle. Their results indicate that no significant reduction in sensitivity is possible for that mission. Both references use optimization schemes that require the guessing of initial values of adjoint variables. In this report, the gradient method, which requires no guessing, is used.

There are a number of error sources which can affect the accuracy of meeting terminal constraints. In general, one would like to find a trajectory which minimizes the sensitivity of all the terminal constraints to all the error sources. The theoretical formulation for solving this problem is given in Section 2. In Section 3 the method is applied to reduce the sensitivity of burnout altitude to first stage burn rate errors for the Scout booster. In Section 4, an investigation is made to determine whether the shape of the trajectory has a significant influence on the sensitivity of the Scout booster to some other major error sources. The trajectory is changed arbitrarily and perturbation runs are made to determine the change in sensitivity.

SECTION 2

GENERAL THEORY

The gradient method of optimization is to be used to reduce error
sensitivities. In order to apply this method, the linear perturbation
equation relating changes in the control variables to changes in the
sensitivity must first be obtained.

The equations of motion for a trajectory can be represented in the
form

$$\dot{x} = f(x, \alpha, \tau, P, q) \tag{1}$$

where   f   is an   n x 1   column vector

   x   is an   n   vector of state variables

   α is an   m   vector of control variables

   τ is an ℓ vector of control parameters

   P   is a   k   vector of system variables

   q   is a   j   vector of system parameters.

The control and system variables are functions which influence the
trajectory over a period of time, while the parameters affect the trajec-
tory at only one time. Thrust attitude and the length of a coast between
powered stages are examples of a control variable and a control parameter,
respectively. The system variables and parameters are the quantities
which cause trajectory errors when they have non-nominal values. The
control variables, once they have been determined, become system variables
because an error in the control is one of the major error sources. Thrust
magnitude and atmosphere density are other examples of system variables and
the burn time of a stage is an example of a system parameter.

The linear perturbation equation relating changes in system variables
and parameters to a terminal constraint is given by (reference 3)

3

$$\delta \psi = \int_{t_i}^{t_f} \Lambda_\psi \delta P dt + S \delta q \qquad (2)$$

where

$\delta \psi$ is the change in the terminal constraint

$$\Lambda_\psi = \lambda_\psi^T \frac{\partial f}{\partial P} \qquad (3)$$

λ_ψ is an n vector of adjoint variables which results from solving the set of differential equations

$$\dot{\lambda}_\psi = -\left(\frac{\partial f}{\partial x}\right)^T \lambda_\psi \qquad (4)$$

with boundary conditions

$$\lambda_\psi(t_f) = \frac{\partial \psi}{\partial x}\bigg|_{t = t_f} \qquad (5)$$

S depends on the parameters being considered. In general, it is a function of x, α, and λ_ψ.

The change in the system variables, dP, will be assumed constant. The sensitivity of the constraint ψ to the variables P is thus given by

$$\frac{d\psi}{dP} = \int_{t_i}^{t_f} \Lambda_\psi dt \qquad (6)$$

and the sensitivity to the parameters q is

$$\frac{d\psi}{dq} = S \qquad (7)$$

$\frac{d\psi}{dP}$ has k components and $\frac{d\psi}{dq}$ has j components. If it is desired to find a trajectory which reduces the sensitivity of the one constraint

4

$\downarrow$ to all the error components, then a weighted sum of the absolute values of the sensitivities must be formed. One obtains

$$\phi = \sum_{i=1}^{k} a_i \left| \frac{d\psi}{dP_i} \right| + \sum_{i=1}^{j} b_i \left| \frac{d\psi}{dq_i} \right| \tag{8}$$

ϕ becomes the payoff quantity to be minimized. The magnitudes of the sensitivities can differ greatly, depending on the system variables and parameters being considered. The weighting coefficients, a_i and b_i, are chosen to equalize the contribution of each term in the payoff. In addition, they can be used to emphasize the importance of certain of the sensitivities.

The absolute value function can be removed from equation (8) by choosing the signs of the weighting coefficients so that the product $a_i \left(\frac{d\psi}{dP_i} \right)$ is always positive. Equation (8) can then be written in the form

$$\phi = \int_{t_i}^{t_f} \Lambda_p dt + S_q \tag{9}$$

where

$$\Lambda_P = \lambda_\psi^T \sum_{i=1}^{k} a_i \frac{\partial f}{\partial P_i} \tag{10}$$

$$S_q = \sum_{i=1}^{j} b_i S_i \tag{11}$$

In general, one will be interested in reducing the effect of the error sources on a number of terminal constraints. Suppose there are c constraints. Then Eqs. (10) and (11) become

5

$$\Lambda_P = \sum_{h=1}^{c} \sum_{i=1}^{k} \lambda_{\psi_h}^T a_{hi} \frac{\partial f}{\partial P_i} \tag{12}$$

$$S_q = \sum_{h=1}^{c} \sum_{i=1}^{j} b_{hi} S_{hi} \tag{13}$$

where λ_{ψ_h} is the vector of adjoint variables associated with the

h^{th} constraint

S_{hi} is the sensitivity of the hth constraint to the ith

parameter

a_{hi} and b_{hi} are matrices of weighting coefficients

The payoff quantity to be minimized is the ϕ of Eq. (9) with Λ_p and S_q taken from Eqs. (12) and (13). ϕ is a function of x, α, and the adjoint variables associated with each terminal constraint. The unique feature of this payoff is the dependence on the adjoint variables. In order to determine the influence of the control on the payoff, one must take into account the change in the adjoint variables as well as the state variables.

The linear perturbation equation relating small changes in the sensitivity payoff to changes in the controls has the form (reference 3)

$$\delta\phi = \int_{t_i}^{t_f} \Lambda_\phi \, \delta\alpha \, dt + S_\phi \delta\tau \tag{14}$$

An expression having this form is obtained by adjoining the state and adjoint differential equations to the equation for the payoff. Following

6

reference 4, form a quantity

$$\overline{F}(t,x,\dot{x},\lambda_{\psi_1},\lambda_{\psi_2}\cdots\dot{\lambda}_{\psi_1},\dot{\lambda}_{\psi_2}\cdots,\alpha) = \Lambda_p(x,\lambda_{\psi_1},\lambda_{\psi_2}\cdots,\alpha)$$

$$+ \nu^T(t)\,(f(x,\alpha)-\dot{x}) + \sum_{h=1}^{c} \mu_h^T(t)\left(\dot{\lambda}_{\psi_h}+(\frac{\partial f}{\partial x})^T\lambda_{\psi_h}\right) \tag{15}$$

$\nu(t)$ and $\mu_h(t)$ are n vectors of adjoint variables or Lagrange multipliers. $\overline{F}$ is just the integrand of Eq. (9) so that

$$\emptyset = \int_{t_i}^{t_f} \overline{F}\ dt + S_q \tag{16}$$

Now, proceeding formally, the differential of $\emptyset$ is given by

$$\delta\emptyset = \int_{t_i}^{t_f}\left[\frac{\partial\overline{F}}{\partial x}\delta x + \frac{\partial\overline{F}}{\partial\dot{x}}\delta\dot{x} + \sum_{h=1}^{c}\left(\frac{\partial\overline{F}}{\partial\lambda_{\psi_h}}\delta\lambda_{\psi_h} + \frac{\partial\overline{F}}{\partial\dot{\lambda}_{\psi_h}}\delta\dot{\lambda}_{\psi_h}\right) + \frac{\partial\overline{F}}{\partial\alpha}\delta\alpha\right]dt$$

$$+ \frac{\partial S_q}{\partial x}\delta x + \sum_{h=1}^{c}\frac{\partial S_q}{\partial\lambda_{\psi_h}}\delta\lambda_{\psi_h} + \frac{\partial S_q}{\partial\alpha}\delta\alpha \tag{17}$$

The partials of S_q are evaluated at the times at which the system parameters influence the trajectory.

The term involving $\delta\dot{x}$ is integrated by parts to give

$$\int_{t_i}^{t_f}\frac{\partial\overline{F}}{\partial\dot{x}}\delta\dot{x}\ dt = \frac{\partial\overline{F}}{\partial\dot{x}}\delta x\Big|_{t_i}^{t_f} - \int_{t_i}^{t_f}\frac{d}{dt}(\frac{\partial\overline{F}}{\partial\dot{x}})\delta x\ dt \tag{18}$$

7

Substituting for $\overline{F}$ from Eq. (15) yields

$$\int_{t_i}^{t_f} \frac{\partial \overline{F}}{\partial \dot{x}} \delta \dot{x}\ dt = \nu^{i^T} \delta x^i - \nu^{f^T} \delta x^f + \int_{t_i}^{t_f} \dot{\nu}^T \delta x\ dt \qquad (19)$$

where the superscripts i and f indicate values at times t_i and t_f, respectively. Similarly, for each of the $\delta \dot{\lambda}_h$ one obtains

$$\int_{t_i}^{t_f} \frac{\partial \overline{F}}{\partial \dot{\lambda}_h} \delta \dot{\lambda}_h\ dt = \mu_h^{f^T} \delta \lambda_h^f - \mu_h^{i^T} \delta \lambda_h^i - \int_{t_i}^{t_f} \dot{\mu}_h^T \delta \lambda_h\ dt \qquad (20)$$

After substituting Eqs. (19) and (20) in Eq. (17), one has

$$\delta \phi = \nu^{i^T} \delta x^i - \nu^{f^T} \delta x^f + \sum_{h=1}^{c} \left(\mu_h^{f^T} \delta \lambda_h^f - \mu_h^{i^T} \delta \lambda_h^i \right)$$

$$+ \int_{t_i}^{t_f} \left[\left(\frac{\partial \overline{F}}{\partial x} + \dot{\nu}^T \right) \delta x + \sum_{h=1}^{c} \left(\frac{\partial \overline{F}}{\partial \lambda_h} - \dot{\mu}_h^T \right) \delta \lambda_h + \frac{\partial \overline{F}}{\partial \alpha} \delta \alpha \right] dt \qquad (21)$$

$$+ \frac{\partial S_q}{\partial x} \delta x + \sum_{h=1}^{c} \frac{\partial S_q}{\partial \lambda_h} \delta \lambda_h + \frac{\partial S_q}{\partial \alpha} \delta \alpha$$

ν and μ_h are selected so that the coefficients of δx and $\delta \lambda_h$ inside the integral are zero. This leads to the differential equations

$$\dot{\nu} = -\left(\frac{\partial \overline{F}}{\partial x} \right)^T \qquad (22)$$

$$\dot{\mu}_h = \left(\frac{\partial \overline{F}}{\partial \lambda_h} \right)^T \qquad h=1, c \qquad (23)$$

8

The boundary conditions for these equations are chosen so that $\delta \phi$ is not a function of unknown quantities. The change in the state at $t_f, \delta x^f$, is unknown. Therefore, its coefficient will be set to zero. This coefficient will involve μ_h^f. Note from Eq. (5) that

$$\delta \lambda_{\psi_h}(t_f) = \frac{\partial}{\partial x}\left(\frac{\partial \psi_h}{\partial x}\right)\delta x^f \tag{24}$$

With Eq. (24) substituted into Eq. (21), the coefficient of δx^f is

$$-\nu^{f^T} + \sum_{h=1}^{c} \mu_h^{f^T} \frac{\partial}{\partial x}\left(\frac{\partial \psi_h}{\partial x}\right)$$

Setting this coefficient to zero leads to the boundary condition for ν.

$$\nu^{f^T} = \sum_{h=1}^{c} \mu_h^{f^T} \frac{\partial}{\partial x}\left(\frac{\partial \psi_h}{\partial x}\right) \tag{25}$$

The adjoint variables, λ_{ψ_h}, are specified at the terminal time. The change in the variables at t_i is unknown. Therefore, the boundary conditions for μ are chosen to be

$$\mu_h^{i^T} = 0 \tag{26}$$

The functions ν and μ_h can be interpreted as sensitivities. $\nu(t)$ gives the change in ϕ due to a change in x at time t. This is identical to the relation between λ_ψ and ψ. $\mu_h(t)$ gives the change in ϕ due to a change in λ_{ψ_h} at time t. Using this interpretation, ν and μ can be modified to include the effects of the system parameters.

Suppose one of the system parameters appears at time t_p. If there

is a δx at time t_p, then by Eq. (21), the sensitivity will change by

$$\frac{\partial S_q}{\partial x} \delta x(t_p)$$

as time goes from t_p^- to t_p^+ . If ν is to be the sensitivity of ϕ to x, then one must introduce a discontinuity in ν at the times when a system parameter affects the trajectory. In a similar manner, a discontinuity in μ_h is introduced at the same times when integrating the μ_h equations.

The presence of the term $\left(\frac{\partial S_q}{\partial \alpha}\right) \delta \alpha$ in Eq. (21) is awkward. If $\delta \alpha$ is the control change, then large changes in ϕ can be made by making large changes in α just at the time the system parameter appears. This will clearly not lead to practical control histories. The solution is to convert α to a state variable and to make $\dot{\alpha}$ the control with a limit on the magnitude of $\dot{\alpha}$. If this is done, the term containing $\delta \alpha$ will become part of the δx term.

Eq. (21), then, is reduced to

$$\delta \phi = \int_{t_i}^{t_f} \frac{\partial \overline{F}}{\partial \alpha} \delta \alpha \, dt \qquad (27)$$

under the following conditions:

1) ν and μ_h satisfy the diffential equations given in Eqs. (22) and (23) with boundary conditions given by Eqs. (25) and (26).

2) The influence of the system parameters is handled by introducing discontinuities in ν and μ_h .

10   10

3) The perturbation in the state variables at $t_i, \delta x^i$, is zero.

Comparing Eq. (27) with Eq. (14), it is seen that the desired influence coefficient, Λ_ϕ, is given by

$$\Lambda_\phi = \frac{\partial \bar{F}}{\partial \alpha} \qquad (28)$$

The effect of the control parameters on the payoff is introduced by taking advantage of the sensitivity interpretation for ν and μ_h. Suppose $\delta\alpha$ is zero from t_i to t_f and introduce non-zero values for δx^i and $\delta\lambda^f_{\psi_h}$. Eq. (21) can then be written as

$$\delta\phi = \nu^{i^T} \delta x^i + \sum_{h=1}^{c} \mu_h^{f^T} \delta\lambda^f_{\psi_h} \qquad (29)$$

A control parameter change, $\delta\tau$, will produce a δx and a $\delta\lambda_{\psi_h}$. S_ϕ is then found from Eq. (29). This procedure will be illustrated in the next section for the case of an adjustable coast between powered stages.

One should perhaps comment on the difference in superscripts for δx and $\delta\lambda_{\psi_h}$ in Eq. (29). The state variables are integrated forward in time. A change δx, applied at time t_i, influences the trajectory forward from t_i to the final time. On the other hand, the adjoint equations are integrated backwards in time. A change $\delta\lambda_{\psi_h}$, applied at time t_f, influences the trajectory backwards from t_f to the initial time.

How do the equations that have been derived here fit into the gradient method of optimization? The initial conditions for the equations involving $\dot{\mu}_h$ (Eq. 23) are specified at t_i. These equations can, therefore, be integrated forward along with the state equations. The

11

initial conditions for the $\dot{v}$ equations (Eq. 22) are given at t_f. These equations, which involve both μ_h and λ_{ψ_h}, are integrated backwards along with the usual adjoint equations (Eq. 4). Λ_ϕ, which is a function of v, μ_h and λ_{ψ_h}, is evaluated and stored along this backward run. Λ_ϕ is combined with the influence coefficients for the terminal constraints in the usual manner and an expression for $\delta\alpha$ which will reduce the payoff while meeting constraints is obtained. Thus, the basic sequence of forward and backward integrations associated with the gradient method is maintained. The only difference is that several additional sets of differential equations must be integrated.

SECTION 3

NUMERICAL EXAMPLE

The procedure described in Section 2 will be used to minimize the sensitivity of terminal altitude to first stage burn rate for the Scout booster. The mission involves placing a payload into a reentry trajectory. There are terminal constraints on the altitude, flight path angle, and down-range location of reentry. There is also a constraint on dynamic pressure at the start of the second stage.

3.1 Assumptions

The Scout Trajectory Optimization and Linearization Program (TØLIP) described in reference 3 has been modified to incorporate sensitivity reduction. In order to reduce the programming complexity, the following simplifications have been made in the model:

(1) Motion is restricted to two dimensions. This reduces the number and complexity of the second-order partial derivatives that must be evaluated.

(2) An exponential atmosphere is used instead of the standard ARDC atmosphere. This makes it possible to evaluate simply the second order partials of density and pressure with respect to altitude.

(3) The lift coefficient is zero and the drag coefficient is assumed to be independent of Mach number. This eliminates the necessity of determining the second order partials of C_L and C_D with respect to Mach number.

(4) The thrust and mass flow rate in the first stage are constant.

The Scout vehicle used for this mission has three stages. The vehicle

13

coasts between the powered stages and the length of each of these coasts is a control parameter. Also, there is no requirement that the third stage burn out at the desired reentry point. Therefore, an adjustable coast is allowed after the third stage. The thrust orientation angle, measured with respect to an inertial coordinate system, is the control variable.

3.2 The Sensitivity Function

The payoff to be minimized is the sensitivity of terminal altitude to first stage burn rate. An increase in the burn rate implies an increase in the thrust and a decrease in the burn time such that the product of thrust and burn time remain constant. The burn rate variation will be represented as a thrust variation where it is understood that a one pound increase in thrust goes along with a decrease in burn time given by the ratio of the nominal burn time to the nominal thrust. Let the nominal stage time be broken up into segments of length dt_n .
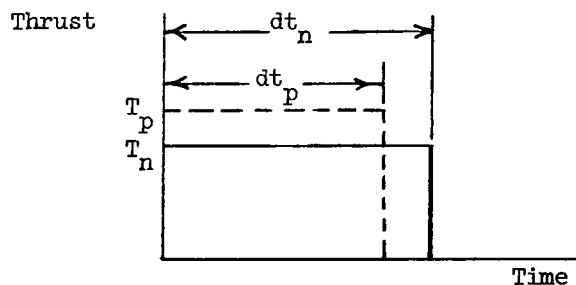

Fig. 1. Sketch of Thrust Histories

The thrust magnitude over each segment is T_n as shown in Figure 1. When the thrust is increased to the perturbed value T_p, the length of each segment is reduced to dt_p .

The change in the terminal altitude, $\delta h \left(t_f \right)$, due to the perturbed thrust over the interval dt_n can be expressed as

14

$$\delta h \, (t_f) = \lambda^T d(\delta x) \qquad\qquad (30)$$

where λ is the vector of adjoint variables associated with the altitude constraint and

$$d(\delta x) = x_p(dt_p) - x_n(dt_n) \qquad\qquad (31)$$

i.e., the difference between the perturbed trajectory variables after time interval dt_p and the nominal variables after time dt_n.

The component of $d(\delta x)$ due to increased thrust is found by writing the differential of the trajectory equations (Eq. 1)

$$\delta \dot{x} = \frac{\partial f}{\partial T} \delta T \qquad\qquad (32)$$

Over the time dt_n, the change in x is

$$d(\delta x_T) = \frac{\partial f}{\partial T} \delta T dt_n \qquad\qquad (33)$$

The burn time is changed by

$$\delta t = \frac{-dt_n}{T_n} \delta T \qquad\qquad (34)$$

If the rate of change of x is f, then $d(\delta x)$ due to the reduced burn time is

$$d(\delta x_t) = - \frac{f}{T_n} \delta T dt_n \qquad\qquad (35)$$

The combined effect is found by adding Eqs. (33) and (35) to give

$$d(\delta x) = \left(\frac{\partial f}{\partial T} - \frac{f}{T_n} \right) \delta T dt_n \qquad\qquad (36)$$

Substituting Eq. (36) into Eq. (30) yields

$$\delta h(t_f) = \lambda^T \left(\frac{\partial f}{\partial T} - \frac{f}{T_n} \right) \delta T dt_n \qquad\qquad (37)$$

The change over an entire stage is found by integrating Eq. (37). The resulting sensitivity is

15

$$\frac{dh}{dT} = \int_{\text{stage 1}} \lambda^T \left(\frac{\partial f}{\partial T} - \frac{f}{T_n}\right) dt \qquad (38)$$

The Λ_p of Eq. (10), then, is just

$$\Lambda_p = \lambda^T \left(\frac{\partial f}{\partial T} - \frac{f}{T_n}\right) \qquad (39)$$

The sensitivity given by Eq. (38) is the payoff in the optimization procedure. In order to determine whether an improvement in payoff has been achieved on a forward run, Eq. (38) must be evaluated. Note, however, that it depends on the adjoint variables evaluated along that trajectory. These adjoint variables are not known until a backward integration of the trajectory has been made. Therefore, at the end of every forward run which meets terminal constraints, a special backward run is made to integrate the adjoint equations so that the payoff can be evaluated.

3.3   The Variational Equations

The sensitivity involves only one terminal constraint so that only one set of μ equations needs to be integrated. These equations are obtained by substituting Eq. (15) into Eq. (23). The result is

$$\dot{\mu} = \frac{\partial f}{\partial x} \mu + \left(\frac{\partial \Lambda_p}{\partial \lambda}\right)^T \qquad (40)$$

From Eq. (26), the initial conditions are seen to be

$$\mu(t_i) = 0 \qquad (41)$$

μ is a five-component vector with one component for each of the state variables, v, γ, r, τ, m. $\partial f / \partial x$ is a 5 x 5 matrix whose components are given in the Appendix. The last term in Eq. (40) is added only during the first stage. From Eq. (39)

16

it is

$$\left(\frac{\partial \Lambda_p}{\partial \lambda}\right)^T = \left(\frac{\partial f}{\partial T} - \frac{f}{T_n}\right) \tag{42}$$

From Eq. (22), the equations for ν are

$$\dot{\nu} = -\left(\frac{\partial \Lambda_p}{\partial x}\right)^T - \left(\frac{\partial f}{\partial x}\right)^T \nu - \left(\frac{\partial}{\partial x}\left[\left(\frac{\partial f}{\partial x}\right)^T \lambda\right]\right)^T \mu \tag{43}$$

with boundary conditions from Eq. (25) equal to

$$\nu(t_f) = 0 \tag{44}$$

ν is a five-component vector. The partial of Λ_p with respect to x is given by

$$\frac{\partial \Lambda_p}{\partial x} = \lambda^T \left(\frac{\partial^2 f}{\partial T \partial x} - \frac{1}{T_n} \frac{\partial f}{\partial x}\right) \tag{45}$$

The quantity in parenthesis in the last term of Eq. (43) is the second-order partial of the Hamiltonian with respect to the state variables.

The influence coefficient relating the control θ to the sensitivity is given by substituting Eq. (15) into Eq. (28). The result is

$$\Lambda_\phi = \frac{\partial \Lambda_p}{\partial \theta} + \gamma^T \frac{\partial f}{\partial \theta} + \mu^T \frac{\partial}{\partial \theta}\left[\left(\frac{\partial f}{\partial x}\right)^T \lambda\right] \tag{46}$$

The partial of Λ_p with respect to θ is given by

$$\frac{\partial \Lambda_p}{\partial \theta} = \lambda^T \left(\frac{\partial^2 f}{\partial T \partial \theta} - \frac{1}{T} \frac{\partial f}{\partial \theta}\right) \tag{47}$$

The final term in Eq. (46) can be written in the form

$$\mu^T \frac{\partial}{\partial \theta}\left[\left(\frac{\partial f}{\partial x}\right)^T \lambda\right] = \mu^T \left[\frac{\partial^2 f}{\partial \theta \partial x}\right]^T \lambda \tag{48}$$

17

The partial derivatives required to evaluate Eqs. (40) to (48) are given in the Appendix.

3.4 Adjustable Coasts

The length of the coast after each powered stage is an adjustable parameter. What influence does a change in coast time have on the sensitivity? Referring to Eq. (29), it is seen that the influence of perturbations in x and λ on the sensitivity ϕ is given by

$$\delta\phi = \nu^T\delta x + \mu^T\delta\lambda \tag{49}$$

where the superscripts of Eq. (29) have been dropped. If the length of a coast is changed on a forward integration, a δx will appear at the end of the coast of magnitude

$$\delta x = \dot{x}\big|_{t_{c_f}}\delta t \tag{50}$$

On the other hand, λ is integrated backwards in time. A change in coast length leads to a $\delta\lambda$ at the beginning of the coast given by

$$\delta\lambda = -\dot{\lambda}\big|_{t_{c_i}}\delta t \tag{51}$$

The combined effect is obtained by substituting Eqs. (50) and (51) into Eq. (49) to give

$$\delta\phi = (\nu^T\dot{x}\big|_{t_{c_f}} - \mu^T\dot{\lambda}\big|_{t_{c_i}})\delta t \tag{52}$$

where t_{c_i} and t_{c_f} represent the times at the beginning and end of coast. The quantity in parenthesis in Eq. (52) is the S_ϕ term of Eq. (14).

3.5 Results

A number of cases were run to determine the reduction in sensitivity
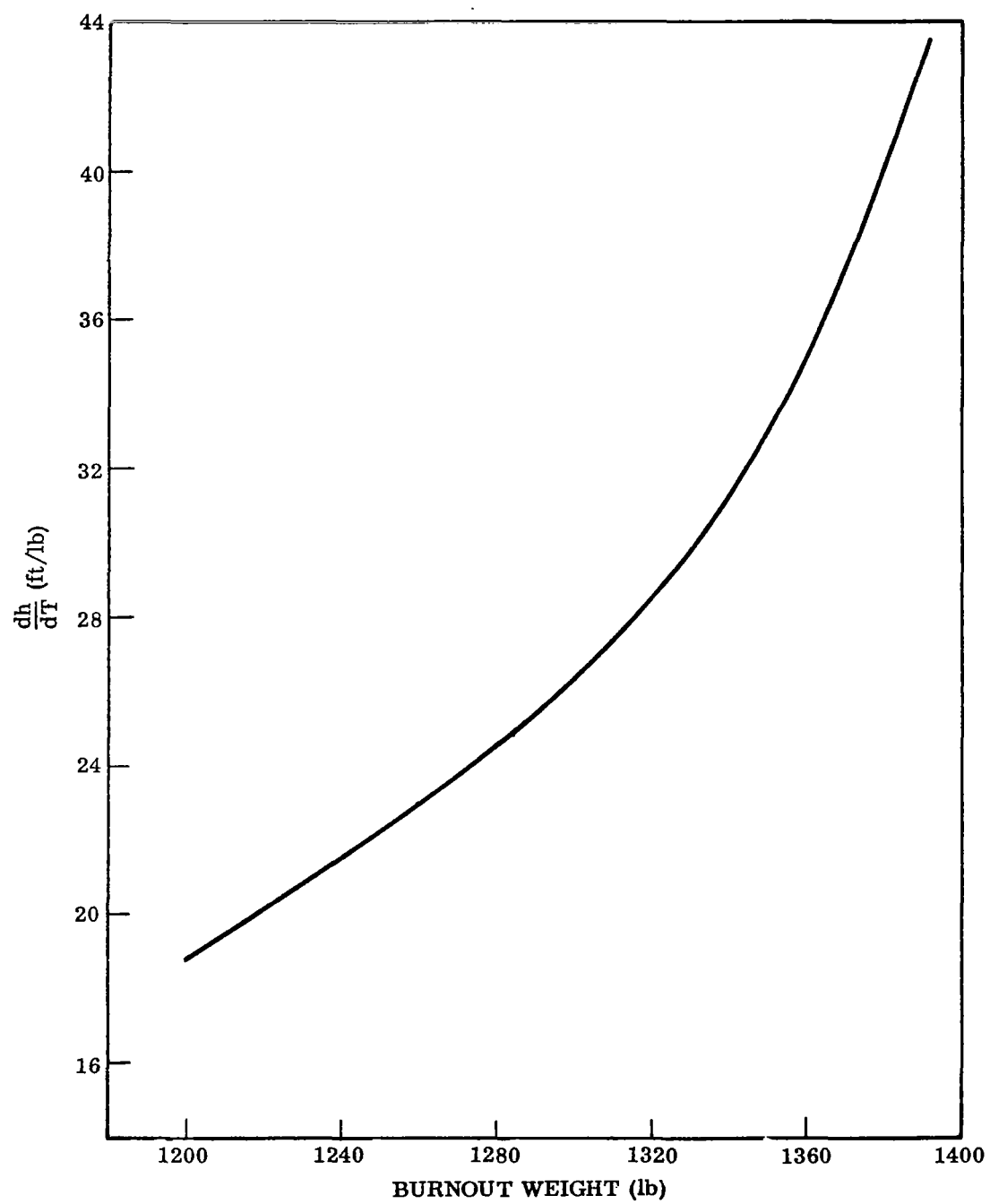
18

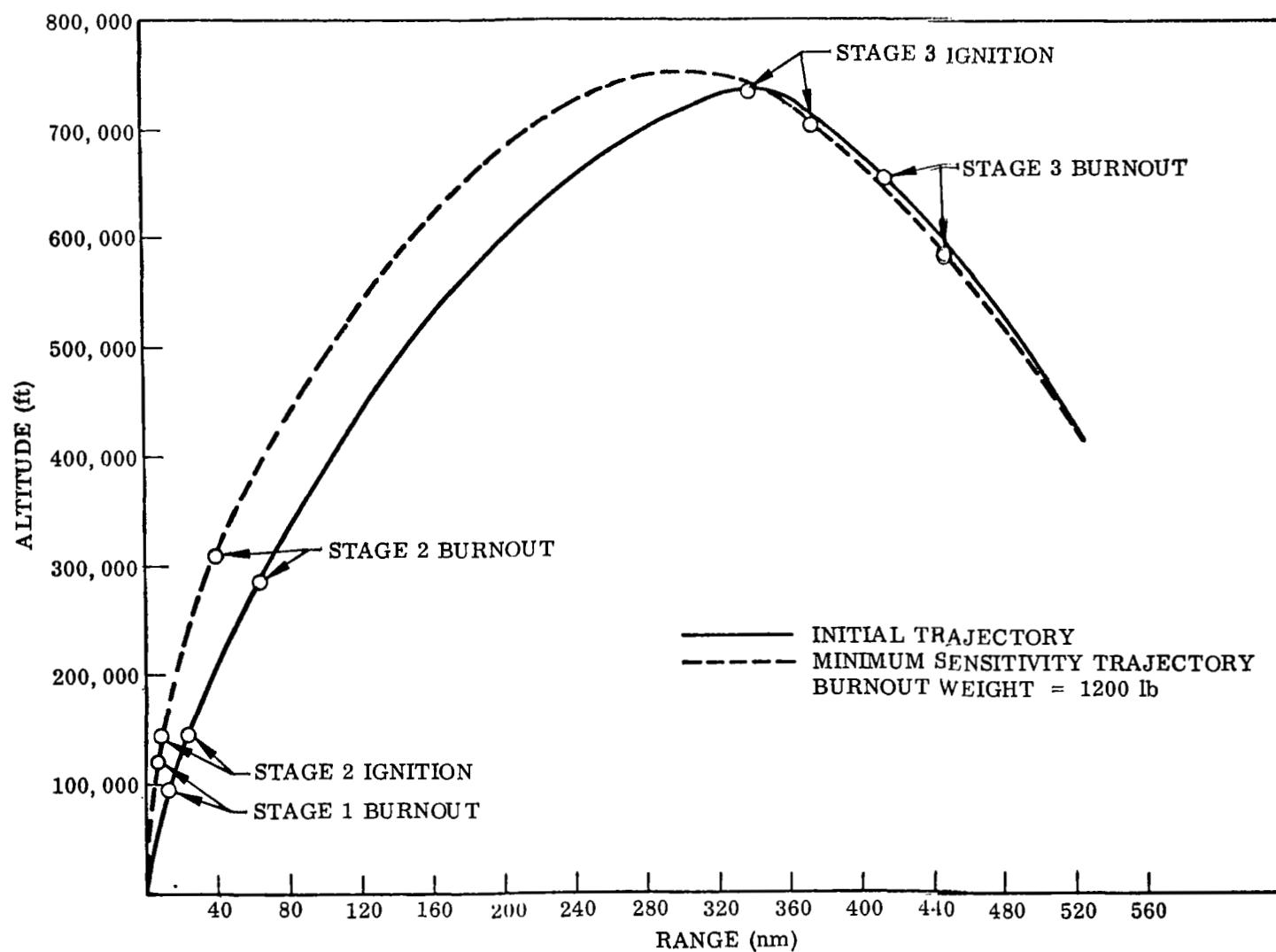Fig. 2 Minimum Sensitivity as a Function of Burnout Weight

Fig. 3 Comparison of Initial and Minimum Sensitivity Trajectories

that can be obtained as the burnout weight is lowered. First,

using the SCOUT optimization program, it was determined that the maxi-

mum burnout weight for the reentry mission is 1392 pounds. The burnout

weight was then fixed at lower values ranging down to 1200 pounds and

the sensitivity was minimized for each burnout weight. As the burnout

weight is lowered, larger changes in the trajectory shape become possible

and the sensitivity can be reduced to a greater degree. The results are

shown in Fig. 2. It is seen that lowering the burnout weight from 1390

to 1200 pounds makes a 50% reduction in sensitivity possible. The general

trend of the trajectory shaping is to steepen the trajectory as shown in

the altitude-range profiles in Fig. 3. The initial trajectory is similar

to the maximum burnout weight trajectory. The control history for the

maximum burnout case was used as the nominal control history for the

1200 pound case. The initial trajectory is the guided trajectory that

met terminal conditions. It should be noted that the sensitivity for

the initial trajectory is 42.3, which is almost as high as the sensi-

tivity for the maximum weight case. This indicates that the reduction

in sensitivity is due to shaping the trajectory and not merely to lower-

ing the burnout weight.

The sensitivities plotted in Fig. 2 come from evaluating the

integral in Eq. (38). To check this integral, the burn rate was per-

turbed for the two trajectories in Fig. 3 and the change in terminal

altitude was observed. A comparison of the integral and the perturba-

tion evaluation of sensitivity is shown in Table 1. The agreement

between the two calculations is good.

TABLE 1

Sensitivity Evaluation

	Integral	Perturbations
Initial trajectory	42.3	43.2
Minimum sensitivity trajectory	18.9	17.3

It is interesting to note that the trajectory that minimizes the altitude sensitivity also reduces the sensitivity of the other terminal constraints to burn rate changes. The effect of a 400 pound change in thrust on the terminal constraints for the two trajectories in Fig. 3 is shown in Table 2.

TABLE 2

Perturbations in Terminal Constraints

Constraint	Initial Trajectory	Minimum Sensivity Trajectory
Altitude (ft)	17276	6901
Flight path angle (dg)	.08	.02
Velocity (fps)	-59.6	-28.3
Range (nm)	-2.3	-1.5

There were several anomalous results that could not be explained. The optimization procedure seemed to converge very well. However, the improvement in payoff that was obtained during early optimization iterations was very close to double the improvement asked for. This behavior has not been noted with conventional payoff variables. Also, perturbation runs were made to check out the velocity and altitude components of the vector ν at the initial time. The results of the perturbation runs differed from the integrated values by a factor of three.

22

SECTION 4

NUMERICAL ERROR SENSITIVITY ANALYSIS

In this section, the results of a numerical analysis of SCOUT error sensitivities are reported. This investigation of the dependence of SCOUT dispersions on the nominal trajectory profile was conducted using the TOLIP computer program (reference 3) originally developed for the NASA SCOUT Project Office at Langley Research Center by LMSC. The SCOUT simulation in TOLIP as employed in the analysis described in this section included the approximated effects of the SCOUT control system characteristics as well as an oblate rotating Earth model. The primary purpose of this analysis was to identify the principal error sources of the SCOUT system and, in particular, find those error sources for which the resultant dispersions could likely be minimized by the automated trajectory shaping procedure discussed in Section 2. To this end, six significant error sources were chosen for study based on the results of the recent TRW SCOUT. Error Analysis Contract (reference 5). These vehicle/environmental anomalies were then simulated on TOLIP to determine resultant dispersion of final burnout conditions. This was done for two different mission trajectory profiles, each of which had been optimized for maximum payload. The nominal trajectories were then offloaded in payload and purposely distorted in such ways as it was felt would reduce dispersions resulting from the same error sources. The dispersed trajectories were then computed about these off-optimum trajectories. As was hoped, error sensitivities were indeed reduced in some cases and Stage 1 burn rate was selected for further study as discussed in Section 3. In the present section, the selection of principal error sources for study, the nominal and distorted trajectories, and a summary of all dispersion results are discussed.

4.1   Nominal Trajectories

In order to study two quite different trajectory profiles a three-stage

23

"Re-entry F" and a five-stage "Sunblazer" case were selected. As shown on the altitude-range profile of Figure 3 the "Re-entry F" configuration employs a two-stage initial boost, coast through apogee, and third stage acceleration to the desired re-entry conditions of velocity, range and flight path angle. A dynamic pressure of 40 lb/ft^2 at stage-two ignition was also imposed. This trajectory has been optimized by TOLIP for maximum payload, producing a third stage burnout weight of 1262.4 lb. The optimum pitch program was automatically linearized by TOLIP, including body dynamics effects. A summary of stage weights used in the simulation is included in Table 3.

The "Sunblazer" configuration which was simulated here employed the same first three stages and a fourth stage assumed to have continuous control, followed by a spin-stabilized final stage. Trajectory constraints imposed on the optimization included the terminal hyperbolic excess velocity, right ascension and declination of the hyperbolic departure asymptote, perigee radius, and dynamic pressure at ignition of stages two and three. The stage weights are summarized in Table 3 Note that maximum stage-five burnout weight is 71.8 lb.

4.2   Dispersion Error Sources

Selection of six principal error sources for study here was based on results of the TRW Error Analysis Contract (reference 5) and a desire to include several different types of vehicle/ environmental anomalies. They are as follows:

— Atmospheric density and pressure variation. Twenty percent high over the entire trajectory, affecting axial and normal force and nozzle back-pressure.

— First stage timer error - first pitch rate step. A delay in the initiation of the pitch-over of 0.234 seconds, all subsequent rates started on time but a residual pitch attitude error of 0.234 $*\dot{\theta}$, over entire trajectory.

24

TABLE 3

SCOUT SUMMARY WEIGHT STATEMENT

	Re-entry F	Sunblazer
Launch Gross	39376.5	39840.9
Stg. 1 Prop.	21355.0	21355.0
Stg. 2 Ignit.	14452.8	14917.2
Stg. 2 Prop.	8275.2	8275.2
Stg. 3 Ignit.	3844.4	4308.8
Stg. 3 Prop.	2582.0	2582.0
(Stg. 3 Burnout)	1262.4	
Stg. 4 Ignit.		946.8
Stg. 4 Prop.		613.9
Stg. 5 Ignit.		265.2
Stg. 5 Prop.		193.4
(Stg. 5 Burnout)		71.8

— First stage specific impulse. Simulated as a 0.54 percent increase in Stage 1 thrust at nominal mass burn-rate.

— First stage burn rate. Simulated as a 4.2 percent increase in thrust and mass burn rate resulting in a 3.22 second shorter duration stage 1 but nominal timing from launch of all other events.

— Second stage thrust misalignment. Simulated as a 0.8 degree pitch-up bias in second stage attitude corresponding to the nominal control system dead band.

— Fifth stage tipoff error. Simulated as a constant pitch-up bias of 2.72 degrees in stage 5 on the "Sunblazer" mission. It should be noted that the magnitudes of all error sources, above, were intended to represent 3 sigma deviations from nominal.

4.3 Error Analysis Results

Summarized in Table 4 are the results of the "Re-entry F" error sensitivity analysis. Errors in third stage burnout velocity, altitude, flight path angle and range are given for the error sources described in Section 4.2. The first set of answers pertains to dispersions about the maximum-payload nominal and are of the same order of magnitude as given in Reference 5. The second set of dispersions are with respect to a distorted nominal in which the same end conditions were met but payload was off-loaded 60 lb. and the first stage trajectory steepened. Flight path angle at first stage burnout was raised from 39 degrees to 50 degrees. Although the expected reduction in sensitivity to atmospheric density and pressure did not materialize, the burn rate sensitivity decreased substantially. Partially on the basis of these results, the burn rate was selected for the work described in Section 3. Another partial set of runs was also made (although not shown in Table 4), in which the first pitch rate was

TABLE 4

"RE-ENTRY F" DISPERSION SUMMARY

Nominal End Conditions: VEL = 19760 ft/sec, ALT = 400,000 ft., GAM =-20 deg., RNG = 525 N.MI.

DISPERSIONS

Error Source	Max. Payload Nom.				Steepened Stg. 1				Minimum Time			
	VEL	ALT	GAM	RNG	VEL	ALT	GAM	RNG	VEL	ALT	GAM	RNG
Atmos Density & Press.	-2	-70,000	-0.73	-5.6	17	-70,000	-0.67	-4.2	1	-66,800	-0.72	-4.9
Timer Error -1st Step	-93	29,900	0.66	-4.4	-107	30,100	0.38	-4.8	-111	34,100	0.44	-4.8
Stg. 1 Spec. Imp.	0	13,600	0.14	1.0	-6	14,800	0.14	0.7	0	12,900	0.13	1.0
Stg. 1 Burnrate	-37	18,300	0.06	-1.1	-20	13,400	0.04	-0.5	-44	19,200	0.05	-1.5
Stg. 2 Thrust Misalin.	-94	28,100	0.14	-3.4	-93	31,600	0.16	-3.4	-94	26,500	0.13	-3.2

set at half the optimum value, thus delaying much of the pitch over. As would
be expected, the dispersions from a timer error at initiation of the first
step were reduced roughly by half. However, other dispersions were virtually
unaffected. On yet another set, second stage burn was delayed somewhat with
the intention of shortening the coast after second stage, thus reducing the
propagation of stage-two thrust misalignment errors. However, the net effect
of forcing a lengthened first coast was in fact to lengthen the second coast,
because of the extra gravity losses introduced, and actually worsen the
dispersions somewhat. In an attempt to profit from this experience, however,
a new option was added to TOLIP to shape trajectories for minimum time to
final burnout. Again, the intent was to directly reduce the propagation time.
As with the steepened first-stage case, the payload was decreased by 60 pounds
and flight time minimized by 20 seconds out of 400. The results are shown
in Table 4, indicating essentially no reduction in sensitivity. Thus, for the
"Re-entry F" mission the most effective means of reducing sensitivities to the
selected error sources was by steepening of the first stage path.

In consideration of the "Sunblazer" mission, again the dispersions about the
maximum payload nominal, steepened first stage, and minimum boost time trajectories
were evaluated. These results are summarized in Table 5, and again one concludes
that an enforced steepening of first stage produces the best results of these
techniques. Here, payload was reduced by only 3 pounds and error sensitivities
were diminished by as much as 30 percent by increasing first stage burnout path
angle from 34 degrees to 50 degrees. For the minimum-time technique the flight
time was reduced from 660 to 520 seconds--again with only a 3 pound payload
reduction. This much reduction in flight time should result in a decreased
sensitivity to many other SCOUT dispersion sources not treated in this analysis.

28

TABLE 5
"SUNBLAZER" DISPERSION SUMMARY

Nominal End Conditions: VEL = 39,586 ft/sec. ALT = 674,000 ft, GAM = 2.50 deg. INCL = 37.9 deg.
Hyperbolic Excess VH = 16,200 ft/sec, RT. ASC.= 85.00 deg. DECLIN. =-36.1 deg.

DISPERSIONS

Error Source	Max. Payload Nom.			Steepened Stg. 1			Minimum Time		
	VH	RT. ASC.	DECLIN.	VH	RT. ASC.	DECLIN.	VH	RT. ASC.	DECLIN.
Atmos Dens. & Press.	-290	1.77	-0.3	-157	1.23	-0.23	-245	1.58	-0.26
Timer Error -1st Step	-217	-0.59	0.11	-163	-0.47	0.08	-201	-0.68	0.12
Stg. 1 Spec. Imp.	52	-0.31	0.05	33	-0.26	0.04	47	-0.29	0.05
Stg. 1 Burn rate	29	-0.05	0.01	-39	0.04	-0.01	-58	0.03	0
Stg. 2 Thrust Misalin.	-134	0.04	-0.01	-105	-0.09	0.01	-120	0.08	-0.01
Stg. 5 Tip-off	4	-1.62	-0.30	5	-1.66	0.31	-250	2.37	-0.39

SECTION 5

CONCLUSIONS AND RECOMMENDATIONS

There are two conclusions to be drawn from this study:

1) Trajectory shaping can significantly reduce the sensitivity of terminal constraints to variations in system parameters.

2) The gradient method of optimization can be used to find the minimum sensitivity trajectory.

In view of the success achieved in minimizing the sensitivity to one error source, it would seen fruitful to apply this method to a problem in which all the major error sources are included simultaneously.

Certain error sources are likely to excite the guidance and control systems of the boost vehicle. The Scout vehicle, for example, will attempt to correct an error in pitch attitude. The behavior of these systems should be included in the model used to evaluate the sensitivities.

APPENDIX

EQUATIONS OF MOTION AND PARTIAL DERIVATIVES

The equations of motion are the two dimensional form of the equations in Ref. 3. They are

$$F = \dot{v} = -g \sin \gamma + \frac{T}{m}(C_{22}\cos\theta + C_{23}\sin\theta) - \frac{D}{m}$$

$$G = \dot{\gamma} = \left(\frac{v}{r} - \frac{g}{v}\right)\cos\gamma + \frac{T}{mv}(C_{32}\cos\theta + C_{33}\sin\theta)$$

$$I = \dot{r} = v \sin\gamma$$

$$K = \dot{\tau} = \frac{v \cos\gamma}{r}$$

$$N = \dot{m} = -\frac{T}{g_o I_{sp}}$$

where

$$C_{22} = \cos\tau \cos\gamma + \sin\tau \sin\gamma$$

$$C_{33} = C_{22}$$

$$C_{23} = -\sin\tau \cos\gamma + \cos\tau \sin\gamma$$

$$C_{32} = -C_{23}$$

$$D = \frac{1}{2}\rho v^2 C_D A \qquad\qquad C_D \text{ independent of Mach number}$$

$$\rho = \rho_o e^{-\beta h} \qquad\qquad\qquad \beta = \frac{1}{23000} \quad .$$

f is a column vector given by

$$f = \begin{bmatrix} F \\ G \\ I \\ K \\ N \end{bmatrix}$$

31

The partial derivative matrix of f with respect to x is

$$
\frac{\partial f}{\partial x} =
\begin{bmatrix}
\frac{\partial F}{\partial v} & \frac{\partial F}{\partial \gamma} & \frac{\partial F}{\partial r} & \frac{\partial F}{\partial \tau} & \frac{\partial F}{\partial m} \\[2ex]
\frac{\partial G}{\partial v} & \frac{\partial G}{\partial \gamma} & \frac{\partial G}{\partial r} & \frac{\partial G}{\partial \tau} & \frac{\partial G}{\partial m} \\[2ex]
\frac{\partial I}{\partial v} & \frac{\partial I}{\partial \gamma} & 0 & 0 & 0 \\[2ex]
\frac{\partial K}{\partial v} & \frac{\partial K}{\partial \gamma} & \frac{\partial K}{\partial r} & 0 & 0 \\[2ex]
0 & 0 & 0 & 0 & 0
\end{bmatrix}
$$

where

$$
\frac{\partial F}{\partial v} = - \frac{1}{m} \rho v A C_D
$$

$$
\frac{\partial F}{\partial \gamma} = -g\,\cos\gamma + \frac{T}{m}\left(\frac{\partial C_{22}}{\partial \gamma}\cos\theta + \frac{\partial C_{23}}{\partial \gamma}\sin\theta\right)
$$

$$
\frac{\partial F}{\partial r} = \frac{2\mu}{r^3}\sin\gamma - \frac{A_e}{m}\frac{dp}{dh}(C_{22}\cos\theta + C_{23}\sin\theta) - \frac{C_D A v^2}{2m}\frac{d\rho}{dh}
$$

$$
\frac{\partial F}{\partial \tau} = \frac{T}{m}\left(\frac{\partial C_{22}}{\partial \tau}\cos\theta + \frac{\partial C_{23}}{\partial \tau}\sin\theta\right)
$$

$$
\frac{\partial F}{\partial m} = - \frac{T}{m^2}(C_{22}\cos\theta + C_{23}\sin\theta) + \frac{D}{m^2}
$$

$$
\frac{\partial G}{\partial v} = \frac{\cos\gamma}{r} + \frac{g}{v^2}\cos\gamma - \frac{T}{mv^2}(C_{32}\cos\theta + C_{33}\sin\theta)
$$

$$
\frac{\partial G}{\partial \gamma} = - \frac{v}{r}\sin\gamma + \frac{g}{v}\sin\gamma + \frac{T}{mv}\left(\frac{\partial C_{32}}{\partial \gamma}\cos\theta + \frac{\partial C_{33}}{\partial \gamma}\sin\theta\right)
$$

$$
\frac{\partial G}{\partial r} = - \frac{v}{r^2}\cos\gamma + \frac{2\mu}{r^3 v}\cos\gamma - \frac{A_e}{mv}\frac{dp}{dh}(C_{32}\cos\theta + C_{33}\sin\theta)
$$

32

$$\frac{\partial G}{\partial \tau} = \frac{T}{mv}\left(\frac{\partial C_{32}}{\partial \tau}\cos\theta + \frac{\partial C_{33}}{\partial \tau}\sin\theta\right)$$

$$\frac{\partial G}{\partial m} = -\frac{T}{m^2 v}(C_{32}\cos\theta + C_{33}\sin\theta)$$

$$\frac{\partial I}{\partial v} = \sin\gamma$$

$$\frac{\partial I}{\partial \gamma} = v\cos\gamma$$

$$\frac{\partial K}{\partial v} = \frac{\cos\gamma}{r}$$

$$\frac{\partial K}{\partial \gamma} = -\frac{v\sin\gamma}{r}$$

$$\frac{\partial K}{\partial r} = -\frac{v\cos\gamma}{r^2}$$

The partial derivatives of f with respect to T are

$$\frac{\partial f}{\partial T} = \begin{bmatrix} \dfrac{\partial F}{\partial T} \\[2mm] \dfrac{\partial G}{\partial T} \\[2mm] 0 \\[2mm] 0 \\[2mm] \dfrac{\partial N}{\partial T} \end{bmatrix}$$

where

$$\frac{\partial F}{\partial T} = \frac{1}{m}(C_{22}\cos\theta + C_{23}\sin\theta)$$

$$\frac{\partial G}{\partial T} = \frac{1}{mv}(C_{32}\cos\theta + C_{33}\sin\theta)$$

33

$$\frac{\partial N}{\partial T} = -\frac{1}{g_o I_{sp}}$$

The second order partial of F with respect to the vector x and the scalar T is found by taking the partial of each term in $\frac{\partial f}{\partial x}$ with respect to T .

$$\frac{\partial^2 f}{\partial T \partial x} = \begin{bmatrix} 0 & F_{T\gamma} & 0 & F_{TT} & F_{Tm} \\ G_{Tv} & G_{T\gamma} & 0 & G_{TT} & G_{Tm} \\ 0 & 0 & 0 & 0 & 0 \\ 0 & 0 & 0 & 0 & 0 \\ 0 & 0 & 0 & 0 & 0 \end{bmatrix}$$

where

$$F_{T\gamma} = \frac{1}{m}\left(\frac{\partial C_{22}}{\partial \gamma} \cos\theta + \frac{\partial C_{23}}{\partial \gamma} \sin\theta\right)$$

$$F_{TT} = \frac{1}{m}\left(\frac{\partial C_{22}}{\partial T} \cos\theta + \frac{\partial C_{23}}{\partial T} \sin\theta\right)$$

$$F_{Tm} = -\frac{1}{m^2}(C_{22}\cos\theta + C_{23}\sin\theta)$$

$$G_{Tv} = -\frac{1}{mv^2}(C_{32}\cos\theta + C_{33}\sin\theta)$$

$$G_{T\gamma} = \frac{1}{mv}\left(\frac{\partial C_{32}}{\partial \gamma} \cos\theta + \frac{\partial C_{33}}{\partial \gamma} \sin\theta\right)$$

$$G_{TT} = \frac{1}{mv}\left(\frac{\partial C_{32}}{\partial T} \cos\theta + \frac{\partial C_{33}}{\partial T} \sin\theta\right)$$

$$G_{Tm} = -\frac{1}{mv^2}(C_{32}\cos\theta + C_{33}\sin\theta)$$

The second order partial of the Hamiltonian is

$$H_{xx} = \frac{\partial}{\partial x}\left[\left(\frac{\partial f}{\partial x}\right)^T \lambda\right]$$

The term in brackets is a column vector. Each component of the vector is converted to a row when the partial with respect to the state vector is taken. The components of H_{xx} can be written as

$$\begin{bmatrix} H_{vv} \\ H_{v\gamma} \\ H_{vr} \\ H_{vT} \\ H_{vm} \end{bmatrix} = \begin{bmatrix} F_{vv} & G_{vv} & 0 & 0 & 0 \\ 0 & G_{v\gamma} & I_{v\gamma} & K_{v\gamma} & 0 \\ F_{vr} & G_{vr} & 0 & K_{vr} & 0 \\ 0 & G_{vT} & 0 & 0 & 0 \\ F_{vm} & G_{vm} & 0 & 0 & 0 \end{bmatrix} [\lambda]$$

$$\begin{bmatrix} H_{\gamma\gamma} \\ H_{\gamma r} \\ H_{\gamma T} \\ H_{\gamma m} \end{bmatrix} = \begin{bmatrix} F_{\gamma\gamma} & G_{\gamma\gamma} & I_{\gamma\gamma} & K_{\gamma\gamma} & 0 \\ F_{\gamma r} & G_{\gamma r} & 0 & K_{\gamma r} & 0 \\ F_{\gamma T} & G_{\gamma T} & 0 & 0 & 0 \\ F_{\gamma m} & G_{\gamma m} & 0 & 0 & 0 \end{bmatrix} [\lambda]$$

$$\begin{bmatrix} H_{rr} \\ H_{rT} \\ H_{rm} \end{bmatrix} = \begin{bmatrix} F_{rr} & G_{rr} & 0 & K_{rr} & 0 \\ F_{rT} & G_{rT} & 0 & 0 & 0 \\ F_{rm} & G_{rm} & 0 & 0 & 0 \end{bmatrix} [\lambda]$$

$$\begin{bmatrix} H_{TT} \\ H_{Tm} \end{bmatrix} = \begin{bmatrix} F_{TT} & G_{TT} & 0 & 0 & 0 \\ F_{Tm} & G_{Tm} & 0 & 0 & 0 \end{bmatrix} [\lambda]$$

$$[H_{mm}] = [F_{mm} \quad G_{mm} \quad 0 \quad 0 \quad 0] [\lambda]$$

where

$$F_{vv} = -\frac{\rho C_D A}{m}$$

35

$$F_{vr} = -\frac{vC_DA}{m}\frac{d\rho}{dh}$$

$$F_{vm} = \frac{\rho vC_DA}{m^2}$$

$$G_{vv} = -\frac{2g\,\cos\gamma}{v^3} + \frac{2T}{mv^3}(C_{32}\cos\theta + C_{33}\sin\theta)$$

$$G_{v\gamma} = -\frac{\sin\gamma}{r} - \frac{g}{v^2}\sin\gamma - \frac{T}{mv^2}\left(\frac{\partial C_{32}}{\partial\gamma}\cos\theta + \frac{\partial C_{33}}{\partial\gamma}\sin\theta\right)$$

$$G_{vr} = -\frac{\cos\gamma}{r^2} - \frac{2\mu}{r^3v^2}\cos\gamma + \frac{A_e}{mv^2}\frac{d\rho}{dh}(C_{32}\cos\theta + C_{33}\sin\theta)$$

$$G_{v\tau} = -\frac{T}{mv^2}\left(\frac{\partial C_{32}}{\partial\tau}\cos\theta + \frac{\partial C_{33}}{\partial\tau}\sin\theta\right)$$

$$G_{vm} = \frac{T}{m^2v^2}(C_{32}\cos\theta + C_{33}\sin\theta)$$

$$I_{v\gamma} = \cos\gamma$$

$$K_{v\gamma} = -\frac{\sin\gamma}{r}$$

$$K_{vr} = -\frac{\cos\gamma}{r^2}$$

$$F_{\gamma\gamma} = g\,\sin\gamma + \frac{T}{m}\left(\frac{\partial^2 C_{22}}{\partial\gamma^2}\cos\theta + \frac{\partial^2 C_{23}}{\partial\gamma^2}\sin\theta\right)$$

$$F_{\gamma r} = \frac{2\mu}{r^3} - \frac{A_e}{m}\frac{d\rho}{dh}\left(\frac{\partial C_{22}}{\partial\gamma}\cos\theta + \frac{\partial C_{23}}{\partial\gamma}\sin\theta\right)$$

$$F_{\gamma\tau} = \frac{T}{m}\left(\frac{\partial^2 C_{22}}{\partial\gamma\partial\tau}\cos\theta + \frac{\partial^2 C_{23}}{\partial\gamma\partial\tau}\sin\theta\right)$$

$$F_{\gamma m} = -\frac{T}{m^2}\left(\frac{\partial C_{22}}{\partial\gamma}\cos\theta + \frac{\partial C_{23}}{\partial\gamma}\sin\theta\right)$$

$$G_{\gamma\gamma} = - \frac{v}{r} \cos\gamma + \frac{g}{v} \cos\gamma + \frac{T}{mv}\left(\frac{\partial^2 C_{32}}{\partial \gamma^2} \cos\theta + \frac{\partial^2 C_{33}}{\partial \gamma^2} \sin\theta\right)$$

$$G_{\gamma r} = \frac{v}{r^2} \sin\gamma - \frac{2\mu}{r^3 v} \sin\gamma - \frac{A_e}{mv}\frac{dp}{dh}\left(\frac{\partial C_{32}}{\partial \gamma} \cos\theta + \frac{\partial C_{33}}{\partial \gamma} \sin\theta\right)$$

$$G_{\gamma\tau} = \frac{T}{mv}\left(\frac{\partial^2 C_{32}}{\partial \gamma \partial \tau} \cos\theta + \frac{\partial^2 C_{33}}{\partial \gamma \partial \tau} \sin\theta\right)$$

$$G_{\gamma m} = - \frac{T}{m^2 v}\left(\frac{\partial C_{32}}{\partial \gamma} \cos\theta + \frac{\partial C_{33}}{\partial \gamma} \sin\theta\right)$$

$$I_{\gamma\gamma} = -v \sin\gamma$$

$$K_{\gamma\gamma} = - \frac{v \cos\gamma}{r}$$

$$K_{\gamma r} = \frac{v \sin\gamma}{r^2}$$

$$F_{rr} = - \frac{6\mu}{r^4} \sin\gamma - \frac{A_e}{m}\frac{d^2 p}{dh^2}(C_{22}\cos\theta + C_{23}\sin\theta) - \frac{v^2 C_D A}{2m}\frac{d^2\rho}{dh^2}$$

$$F_{r\tau} = - \frac{A_e}{m}\frac{dp}{dh}\left(\frac{\partial C_{22}}{\partial \tau} \cos\theta + \frac{\partial C_{23}}{\partial \tau} \sin\theta\right)$$

$$F_{rm} = \frac{A_e}{m^2}\frac{dp}{dh}(C_{22}\cos\theta + C_{23}\sin\theta) - \frac{C_D A v^2}{2m^2}\frac{d\rho}{dh}$$

$$G_{rr} = \frac{2v}{r^3} \cos\gamma - \frac{6\mu}{r^4 v} \cos\gamma - \frac{A_e}{mv}\frac{d^2 p}{dh^2}(C_{32}\cos\theta + C_{33}\sin\theta)$$

$$G_{r\tau} = - \frac{A_e}{mv}\frac{dp}{dh}\left(\frac{\partial C_{32}}{\partial \tau} \cos\theta + \frac{\partial C_{33}}{\partial \tau} \sin\theta\right)$$

$$G_{rm} = \frac{A_e}{m^2 v}\frac{dp}{dh}(C_{32}\cos\theta + C_{33}\sin\theta)$$

$$K_{rr} = \frac{2v}{r^3} \cos\gamma$$

$$F_{\tau\tau} = \frac{T}{m}\left(\frac{\partial^2 C_{22}}{\partial \tau^2} \cos\theta + \frac{\partial^2 C_{23}}{\partial \tau^2} \sin\theta\right)$$

$$F_{\tau m} = - \frac{T}{m^2}\left(\frac{\partial C_{22}}{\partial \tau}\cos\theta + \frac{\partial C_{23}}{\partial \tau}\sin\theta\right)$$

$$G_{\tau\tau} = \frac{T}{mv}\left(\frac{\partial^2 C_{32}}{\partial \tau^2}\cos\theta + \frac{\partial^2 C_{33}}{\partial \tau^2}\sin\theta\right)$$

$$G_{\tau m} = - \frac{T}{m^2 v}\left(\frac{\partial C_{32}}{\partial \tau}\cos\theta + \frac{\partial C_{33}}{\partial \tau}\sin\theta\right)$$

$$F_{mm} = \frac{2T}{m^3}(C_{22}\cos\theta + C_{23}\sin\theta) - \frac{2D}{m^3}$$

$$G_{mm} = \frac{2T}{m^3 v}(C_{32}\cos\theta + C_{33}\sin\theta)$$

The partial of F with respect to θ is

$$\frac{\partial f}{\partial \theta} = \begin{bmatrix} \dfrac{\partial F}{\partial \theta} \\[2mm] \dfrac{\partial G}{\partial \theta} \\[2mm] 0 \\[1mm] 0 \\[1mm] 0 \end{bmatrix}$$

where

$$\frac{\partial F}{\partial \theta} = \frac{T}{m}(-C_{22}\sin\theta + C_{23}\cos\theta)$$

$$\frac{\partial G}{\partial \theta} = \frac{T}{mv}(-C_{32}\sin\theta + C_{33}\cos\theta)$$

The second order partial of f with respect to the scalars T and θ is

$$\frac{\partial^2 f}{\partial T \partial \theta} = \begin{bmatrix} \dfrac{\partial^2 F}{\partial T \partial \theta} \\[2mm] \dfrac{\partial^2 G}{\partial T \partial \theta} \\[1mm] 0 \\[1mm] 0 \\[1mm] 0 \end{bmatrix}$$

where

$$\frac{\partial^2 F}{\partial T \partial \theta} = \frac{1}{m}(-C_{22}\sin\theta + C_{23}\cos\theta)$$

$$\frac{\partial^2 G}{\partial T \partial \theta} = \frac{1}{mv}(-C_{32}\sin\theta + C_{33}\cos\theta)$$

The second order parital of f with respect to x and θ is found by taking the derivative of each component of $\frac{\partial f}{\partial x}$ with respect to θ

$$\frac{\partial^2 f}{\partial \theta \partial x} = \begin{bmatrix} 0 & F_{\theta\gamma} & F_{\theta r} & F_{\theta T} & F_{\theta m} \\ G_{\theta v} & G_{\theta\gamma} & G_{\theta r} & G_{\theta T} & G_{\theta m} \\ 0 & 0 & 0 & 0 & 0 \\ 0 & 0 & 0 & 0 & 0 \\ 0 & 0 & 0 & 0 & 0 \end{bmatrix}$$

where

$$F_{\theta\gamma} = \frac{T}{m}\left(-\frac{\partial C_{22}}{\partial \gamma}\sin\theta + \frac{\partial C_{23}}{\partial \gamma}\cos\theta\right)$$

$$F_{\theta r} = -\frac{A_e}{m}\frac{dp}{dh}(-C_{22}\sin\theta + C_{23}\cos\theta)$$

$$F_{\theta T} = \frac{T}{m}\left(-\frac{\partial C_{22}}{\partial T}\sin\theta + \frac{\partial C_{23}}{\partial T}\cos\theta\right)$$

$$F_{\theta m} = -\frac{T}{m^2}(-C_{22}\sin\theta + C_{23}\cos\theta)$$

$$G_{\theta v} = -\frac{T}{mv^2}(-C_{32}\sin\theta + C_{33}\cos\theta)$$

$$G_{\theta\gamma} = \frac{T}{mv}\left(-\frac{\partial C_{32}}{\partial \gamma}\sin\theta + \frac{\partial C_{33}}{\partial \gamma}\cos\theta\right)$$

$$G_{\theta r} = -\frac{A_e}{mv}\frac{dp}{dh}(-C_{32}\sin\theta + C_{33}\cos\theta)$$

$$G_{\theta\tau} = \frac{T}{mv}\left(-\frac{\partial C_{32}}{\partial \tau}\sin\theta + \frac{\partial C_{33}}{\partial \tau}\cos\theta\right)$$

$$G_{\theta m} = -\frac{T}{m^2 v}(-C_{32}\sin\theta + C_{33}\cos\theta)$$

REFERENCES

1. Leondes, C. T. and Volgenau, E., "Improvement of Missile and Space Vehicle Accuracy by Trajectory Optimization", J. Spacecraft Rockets 4, 1609-1612, (1967).

2. Watson, J. W. and Stubberud, A. R., "Atmospheric Entry Employing Range Sensitivity", J. Spacecraft Rockets 5, 983-984 (1968).

3. TOLIP - Trajectory Optimization and Linearized Pitch Computer Program, Sections 5 and 8, NASA CR 66515 (1967).

4. Breakwell, J. V., "The Optimization of Trajectories", SIAM J. 7, 215-247 (1959).

5. Scout Error Analysis, CR 66596 and CR 66674 (TRW).